RSC Publishing Faraday Discussions

Unique selectivity trends of highly permeable PAP[5] water channel membranes

Journal:	*Faraday Discussions*
Manuscript ID	FD-ART-02-2018-000043.R1
Article Type:	Paper
Date Submitted by the Author:	03-Apr-2018

Complete List of Authors:	Song, Woochul; Pennsylvania State University, Chemical Engineering Shen, Yue-xiao; University of California Berkeley, Chemistry Lang, Chao; Pennsylvania State University, Chemical Engineering Saha, Prantik; Tufts University - Boston Campus, Physics and Astronomy Zenyuk, Iryna; Tufts University, Mechanical Engineering Hickey, Robert ; Pennsylvania State University, Materials Science and Engineering; Pennsylvania State University Kumar, Manish; The Pennsylvania State University, Department of Chemical Engineering; Pennsylvania State University, Biomedical Engineering; Pennsylvania State University, Civil and Environmental Engineering

Unique selectivity trends of highly permeable PAP[5] water channel membranes

Woochul Song[1], Yue-xiao Shen[2], Chao Lang[1], Prantik Saha[3], Iryna V. Zenyuk[4], Robert J. Hickey[5] and Manish Kumar[*1,6,7]

[1] Department of Chemical Engineering, [5]Department of Materials Science and Engineering, [6] Department of Biomedical Engineering, [7] Department of Civil and Environmental Engineering, The Pennsylvania State University, University Park, PA, 16802 USA
[2] Department of Chemistry, University of California, Berkeley, CA, 94720 USA
[3]Department of Physics and Astronomy, [4]Department of Mechanical Engineering, Tufts University, Medford, MA, 02155 USA

*To whom correspondence should be addressed. Tel.: (814)-865-7519; Email: manish.kumar@psu.edu

Abstract

Artificial water channels are a practical alternative to biological water channels for achieving exceptional water permeability and selectivity in a stable and scalable architecture. However, channel-based membrane fabrication faces critical barriers such; 1) increasing pore density to achieve measurable gains in permeability while maintaining selectivity, and 2) scale-up to practical membrane sizes for applications. Recently, we proposed a technique to prepare channel based membranes using peptide-appended pillar[5]arene (PAP[5]) artificial water channels, addressing the above challenges. These multi-layered PAP[5] membranes (ML-PAP[5]) showed significantly improved water permeability compared to commercial membranes with similar molecular weight cut-offs. However, due to the distinctive pore structure of water channels and the layer-by-layer architecture of the membrane, the separation behavior is unique and was still not fully understood. In this paper, two unique selectivity trends of ML-PAP[5] membranes are discussed from the perspectives of channel geometry, ion exclusion, and linear molecule transport.

Introduction

Water channel based membranes are emerging as innovative materials to improve the performance of current polymeric membranes by enhancing both permeability and selectivity.[1, 2] Artificial water channel research has seen significant progress during the last 5 years, including the development of channels that have comparable water permeability or selectivity to biological water channels.[3-5] These recent advances in developing synthetic water channels have led to the development of the first practical channel based membranes. We recently proposed a strategy to prepare highly permeable water channel based membranes using peptide-appended pillar[5]arene (PAP[5]) synthetic water channels using a layer-by-layer deposition technique to create multiple layers of PAP[5]-rich poly(butadiene)-poly(ethylene oxide) (PB-PEO) block copolymer sheets (**Figure 1**). We also demonstrated that the molecular transport properties of PAP[5] water channels can be successfully preserved in practical pressure driven membrane configurations.[6] These multilayered PAP[5] (ML-PAP[5]) membranes have thin selective layers on top of porous support membranes, where the selective layers are composed of multi layered PAP[5]/PB-PEO block copolymer nanosheets. These multi-layered PAP[5] membranes demonstrated a molecular weight cut-off of ~500 Da, which corresponds well with PAP[5] water channel's intrinsic molecular exclusion properties.[4] Compared to commercial nanofiltration membranes which have similar separation (molecular weight cut-off, MWCO) properties, ML-PAP[5] showed an order of magnitude higher water permeability while maintaining selectivity similar to these membranes.[6] However, due to the unique structure of channel-based membranes and the use of a layer-by-layer architecture, their intrinsic separation properties have not been fully understood.

In this work, the unique separation properties of ML-PAP[5] membranes are explored. In our previous study, successful integration of water channels into practical membranes has been demonstrated, showing distinctive size based exclusion properties which are preserved all the way from the single channel scale.[6] However, due to the layer-by-layer integration of such channels, which results in electrostatic multilayers, characteristic cation selectivity is seen at low ionic concentration environments. Further, while characterization of membranes with rigid molecules such as dyes provided a MWCO of ~600 Da, transmission of poly(ethylene oxide) (PEO) oligomers of weights up to 4000 Da was observed. We hypothesize that this transmission of linear molecules is a distinctive property of channel-based membranes, which have cylinder-like pore structures that span the entire length of the selective layer.

Experimental Methods

Preparation of ML-PAP[5] membranes

ML-PAP[5] membranes were prepared as described elsewhere.[6] Briefly, this process includes three steps: 1) assembly of PAP[5] channels into tightly packed and vertically aligned 2D sheet structures of ~1 micron scale, 2) formation of selective multilayers on microporous support membranes by alternating depositions of poly(ethylenimine) (PEI) polymers and 2D sheets, and 3) chemical crosslinking between PEI and 2D sheets layers to confer mechanical stability against imposed hydraulic pressure.

Membrane evaluation

ML-PAP[5] membranes were evaluated in terms of water permeability and selectivity by dead-end stirred filtration. Hydraulic permeability was estimated using the following equation,

$$L_p = \frac{J_v}{\Delta P} \quad (1)$$

where L_p is hydraulic permeability ($\mathrm{L \cdot m^{-2} \cdot h^{-1} \cdot bar^{-1}}$, LMH/bar), J_v is volumetric flux of

water ($\mathrm{L \cdot m^{-2} \cdot h^{-1}}$, LMH) and ΔP is applied pressure (bar) difference across the membrane. Membranes were tested at 70 psi and volumetric flow rates were measured after they became consistent with filtration time. Solute rejection tests were carried out with different sets of molecules with various molecular weights or ionic valence ratios, including organic dyes (35 μM), ionic salts (0.5 mM) and PEO oligomers (1 g/L). Rejection of each solute was calculated based on the equation,

$$R = \left(1 - \frac{C_P}{C_F}\right) \times 100 \quad (2)$$

where R is rejection of solute (%), C_P and C_F are solute concentrations in permeate and feed solutions respectively. Concentrations of ions, organic dyes and PEO oligomers were measured using conductivity measurements, UV-VIS spectrometry, and a total organic carbon analyzer, respectively.

Results and discussions

Selectivity mechanisms of ML-PAP[5] membrane; size exclusion vs. electrostatic interaction

In our previous study, ML-PAP[5] membranes showed MWCO as ~500 Da in good agreement with single channels' size-exclusive selectivity that were estimated from stopped-flow experiments (~420 Da).[4, 6] The MWCO of this membrane was carefully evaluated by pressure driven filtration experiments with various molecular weights of organic dyes. However, with regard to this experimental result, an important question to address was whether the molecular sieving effect originates from size exclusion of channels or electrostatic interactions between solutes and layered membrane structures, because most water-soluble organic dyes are charged.

In order to identify the ML-PAP[5] membranes' solute exclusion mechanism, dye rejection tests were carried out under various ionic strength environments. If the electrostatic interactions are the main mechanism for exclusions, the rejections would be severely affected by ionic strength of solution due to the electrostatic screening effect.[7] For this experiment, methyl blue was chosen as a subject solute owing to the similarity in its molecular weight (~750 Da) to the membrane's MWCO (~500 Da). The ionic strength of the feed solution was adjusted from 0.035 to 200 mM using sodium chloride (NaCl). The ML-PAP[5] membranes did not show significant rejection decrease at the highest ionic strength condition, maintaining more than 85 % of dye rejection (**Figure 2A**). Also, this result indicates that the rejections are independent on the Debye length (λ_D) of the ionic solutions (**Figure 2B**). λ_D is a parameter that describes how far electrolytes' electrostatic effects can be sustained from the subjects' surfaces in electrolyte solutions.[7] Using this property, Fornasiero *et al*. studied the relationship between λ_D and ion exclusion behavior of electrochemically modified carbon nanotube membranes, and they demonstrated that the solute rejections almost disappear as λ_D becomes close to the pore diameter, if charged species exclusion occurs mostly by electrostatic interactions.[7] In case of our experiments, the λ_D was 0.48 nm for the 200 mM ionic strength condition, which is very comparable with the pore size of PAP[5] channel (~0.5 nm). Nonetheless, the dyes were effectively excluded by the ML-PAP[5] membranes even under these conditions (**Figure 2B**), implying that the electrostatic interactions did not play an significant role in selective properties of the ML-PAP[5] membranes for the macromolecular dyes, which had been used for estimating the MWCO. Consequently, the size dependent exclusion is the dominant factor for this membrane at these molecular scales.

Point-charged ion exclusion by ML-PAP[5] membrane

We also studied ion exclusion by ML-PAP[5] membranes at low ionic strengths to understand how electrostatic layered structures affect ion exclusion properties, especially in low ionic concentration environments. Note that no significant ionic exclusion was shown at ionic strengths greater than 35 mM which are similar to standard conditions for testing conventional nanofiltration (NF) or reverse

osmosis (RO) membranes, due to the large pore size of the channels compared to ionic species.[6]

Ion exclusion via electrostatic interactions between ions and charged membranes has been well described by the Donnan exclusion effect.[8] This theory describes the electrochemical solute behavior at the interface of charged membranes and ionic solutions. In general, the charged membrane builds opposite charge gradients over the membrane surface and, as a result, presents electrostatic potentials from the membrane surface to the bulk phase of the ionic solution, which is called Donnan potential.[7-9] As a result, even under the pressure driven filtration, some ions cannot overcome this potential resulting in ionic exclusion. Also, the counter ions will potentially be rejected at the same time, if they cannot compensate for the energy requirement, which is needed to separate the ion pairs. The rejection coefficient resulting from Donnan exclusion is described by the following equation:[10]

$$R = 1 - \left(\frac{|z_i|c_i}{|z_i|{c_i}^m + {c_x}^m}\right)^{|z_i/z_j|} \quad (3)$$

where c_i and ${c_i}^m$ are co-ion (same charge ions with membrane) concentrations of solution and membrane, ${c_x}^m$ is the charge concentration of the membrane, i and j represents the opposite charge signs, and z is the ionic valence number. ${c_i}^m$ is generally adapted as the co-ion concentration of the permeate solution.[10]

From the structural point of view, the selective layer of the ML-PAP[5] membrane has two oppositely charged layers, which can be effective for ionic exclusion; one is the channel based nanosheet layer which is negatively charged and the other is the positively charged PEI layer (**Figure 1**). The nanosheet layers are highly functionalized with -COOH reactive groups on both the channel entrances and PEO ends, representing the negatively charged layers. On the other hand, the PEI polymers possess a number of -NH_2 groups, which result in positive charges at circumneutral pH. Both reactive groups were introduced to be crosslinked with each other to confer enough mechanical stability onto the entire selective layer.[6] However, this resulted in charged layer-by-layer structures.

To understand whether the ML-PAP[5] membrane has ionic selectivity at low ionic strength and, if it does, what charge interactions are responsible for the electrostatic exclusion, several salts with different ionic valence ratios were tested and the rejection trend was compared with that predicted by the Donnan equilibrium equation (1). The ionic exclusion measurement showed a trend of increasing rejection along with the increasing ratios of positive to negative valence numbers (**Figure 3A**), indicating that positively charged layers are responsible for the ionic rejections. This result is counter intuitive because the outermost top layer of the ML-PAP[5] membrane is composed of negatively charged nanosheets and our expectation was that this top layer would have dominant impact on the observed ionic rejection trends. However, this experimental result suggested to us that, even though the electrostatic potential can be constructed by both PEI and nanosheet layers respectively, the net surface potential is dominated by a positively charged PEI layers and results in multi-valent anionic selectivity (**Figure 4A**). We confirmed this hypothesis by conducting surface zeta-potential (ξ, mV) measurements of ML-PAP[5] membranes (**Figure 4B and 4C**) which indicated that the ML-PAP[5] membranes have a positive zeta potential, despite the presence of outer most layer of negative charged PAP[5] nanosheets.

In order to further confirm that the PEI layers were indeed responsible for cation selectivity under low ionic concentrations, the support polycarbonate membranes with only PEI layers were also tested for ionic salt rejections (**Figure 3B**). In spite of the large pore size of support membrane (50 nm), they showed 60 – 80% ion exclusion compared to ML-PAP[5] membranes. Also, the ML-PAP[5] membranes with additional PEI layer on the top showed similar ion rejection trends to ML-PAP[5] membranes, indicating the large impact of PEI layers in terms of ion rejection rather than PAP[5] channel layers. Based on these results, theoretical ionic rejections were calculated using equation (1)

and compared with the experimental results. The charge concentration of the membrane ($c_x{}^m$) is estimated as 3.5 mM by fitting the experimental rejection data of tris(bipyridine)ruthenium(III) chloride ($Ru(bipy)_3Cl_2$) into the equation (1). As expected, the theoretical Donnan rejections displayed good agreement with experimental values (**Figure 3A**).

Linear molecule passage through cylindrical pore via elongational flow

Linear and flexible polymer chains have been known to permeate through cylindrical or conical pores that are much smaller than the expected polymer dimensions in aqueous solutions.[11-14] This passage phenomenon has been explored in a number of studies and has implications in fields ranging from polymer physics to practical downstream membrane bioseparations.[11-20] The phenomenon of linear molecule flow through small pores is based on polymer deformation which is accompanied by elongational flow of the solvent, leading to polymers' entrance into pores. Flexible polymers in the dilute regime (when the polymer concentration is less than the chain overlap concentration) maintain thermodynamically stable conformations, and this results in globular (folded chain) shapes with predictable radii of gyration (R_g). Thus, from the geometric perspective, if the R_g is larger than the radius of pores (R_p), polymers are not able to flow through the pores. However, many empirical experiments have shown that under certain conditions, linear polymers can flow through the pores even though the R_p is substantially smaller than R_g. Specifically, under the filtration environment, when the polymers get closer to the pore entrances along with the solvent flow, two compensating factors compete with each other resulting in the final polymer conformation that dictates whether the polymer enters and passes through the pores (**Figure 5A**). One is elongational shear stress (stretching force) and the other is polymer relaxation (restoration force). The shear force originates from convergent flow of solvent near the pore entrance, while polymer relaxation is a result of Brownian fluctuations of the polymers. If the polymers can be stretched out as a result of shear rate overcoming the relaxation force, then they can flow through the pores; this polymer deformation phenomenon is called affine.[21] In the opposite situation where the shear rate cannot overcome the relaxation force, the polymers exist as thermodynamically stable globule shapes and can't pass through the pores. With respect to this phenomenon, the critical share rate (S_c) has been described as

$$S_c \cong {\tau_z}^{-1} \cong \frac{k_B T}{\eta {R_g}^3} \quad (4)$$

where τ_z is the Zimm relaxation time of the polymers, k_B is the Boltzmann constant, T is the absolute temperature and η is the viscosity of the solution.[22] Daoudi and Brochard correlated this equation with membrane performances and suggested a critical flux (J_c) equation, which describes the minimum hydraulic flux to attain S_c that allows for entrance of the polymers into the pore along with solvent flow.[12]

$$J_c = \frac{k_B T}{\eta} \quad (5)$$

Although this equation is based on a number of assumptions such as perfectly circular and uniform pore shapes, and no interferences in convergent flows between neighboring pores, this critical flux equation has led many other derived critical flux equations that are reasonably applicable in various membrane applications.[15, 16] Furthermore, the work by Daoudi and Brochard suggests that any flexible linear polymer chain in the dilute regime, no matter the molecular weight, such PEO will pass through a cylindrical pore when the elongational shear reaches a critical value.[12] For the stated reasons, it is highly possible for linear polymer chains to pass through the PAP[5] channels, as will be described within the following section.

PEO transmission across ML-PAP[5] membrane through PAP[5] channel's straight through pores

ML-PAP[5] membranes were tested with PEO polymers to confirm that the molecular sieving effect of the ML-PAP[5] membranes is irrespective of charge effects. However, repeated experiments revealed that PEO polymers of sizes several times larger than the determined exclusion limit of the membrane (500 Da) could not be significantly rejected by the ML-PAP[5] membranes, regardless of wide range of oligomer molecular weights (**Figure 5B**). Contrary to the channel based membranes, current NF membranes with similar MWCOs to the ML-PAP membranes have an active layer which is commonly considered non-porous and expected to have voids that are only connected transiently due to thermal motion of the polymers.[1, 23] For these membranes, use of linear molecules such as PEO and poly(propylene oxide) seem to work well, and are established standards in many protocols for MWCO determination.[24, 25] On the other hand, channel based ML-PAP[5] membranes have cylindrical, straight through pores spanning the entire selective layer. Thus, considering the PEO's flexibility as well as linearity, we hypothesized that linear molecule transmission could be a distinctive property of channel-based membranes, which has been mostly seen in the ultrafiltration membrane applications up to date. To rationally presume the possibility of this hypothesis, the theoretical critical flux (J_c) was calculated (see the supplementary information for detailed calculation), and then compared with actual experimental water flux. However, the experimental water flux (0.223 mol/m^2·s) was significantly lower than the theoretical critical flux (296,000 mol/m^2 ·s), implying that the PEO molecules cannot be sufficiently stretched out under this experimental (hydraulic flux) condition and cannot pass through the channel pores.

Another possible hypothesis that could explain PEO transmission through ML-PAP[5] membrane is to consider possible mutual interactions between PEO oligomers and ML-PAP[5] membrane matrix. As shown in **Figure 5A**, the PAP[5] water channels are structurally supported by PB-PEO block copolymers. Consequently, very dense PEO brushes face the feed solution side and surround channel entrances. Therefore, it would be worthwhile to consider potential intermolecular interactions between PEO oligomers and PEO matrix, which can have an influence on the observed PEO passage trends. Most current elongational flow models do not consider the effect of intermolecular interactions on polymer deformations as most of practical membrane applications involve operations at dilute polymer concentrations. However, Brochard and Neel suggested that, in case of semi-diluted or highly concentrated polymer solutions, intermolecular interactions could result in significant effect on polymer deformation and passage through the pore.[12, 14] For example, if the polymer coils are overlapped with each other in concentrated environments, the polymer relaxation time (τ_z) would be greater than that of diluted polymers due to the steric hindrance of very closely spaced polymers and, as a consequence, result in significantly reduced critical shear rate of polymers (see equation (2)). Based on this approach, Brochard and Neel suggested a corrected critical flux equation (J_c^*) for concentrated polymer solutions as

$$J_c^* = \frac{k_B T}{\eta}\left(\frac{C^*}{C}\right)^{\frac{15}{4}} \quad (6)$$

where C^* and C are the polymer overlap concentration and polymer concentration in feed solution respectively.[12, 14] This equation indicates that if the polymer concentration is higher than the corresponding polymers' overlap concentration, the polymers can suffer the chain deformation much easily even under the mild shear stress environments, and this results in dramatically lowered critical flux. Based on this approach, we hypothesize it is possible that, when PEO polymer chains get closer to PEO brushes along with convergent flow of water, they can be easily stretched out owing to the surrounding dense PEO brushes and are able to pass through the channel pores with water flow. However, since there are a number of assumptions inherent to the current analyses, further studies will be needed to confirm the proposed hypothesis.

Conclusion

Several unique selectivity trends were observed for a new class of channel-based membranes. It was previously demonstrated that for ML-PAP[5] membranes size-exclusion and permeability of the individual water channel can be successfully preserved even at practical membrane scales. Here we attribute a characteristic ion selectivity trend at low ionic strengths that is attributable to the membrane structure rather than channel's characteristics. These results suggest several new aspects that need to be considered in designing practical channel based membranes. During the last few years, the relationships between channels and their molecular transport behaviors have been carefully studied, however, only the importance of the channels' properties has been emphasized in most cases. An emerging emphasis of current channel research is on synthesizing practical membranes, therefore, it would be worthwhile to consider the channel-based membranes more systemically, from the unitary properties of the channels to the entire membrane system. In addition, due to the intrinsic and very distinctive cylinder like pore structures of water channels, the transport phenomenon is difficult to anticipate just based on the consideration of transport in current solution diffusion thin film composite membranes. Therefore, addressing this knowledge gap would be necessary to fully understand the potential advantages and drawbacks of channel based membranes for future applications.

Conflicts of interests

There are no conflicts of interest to declare.

Acknowledgements

We thank to Dr. Michael Hickner, Pennsylvania State University, to provide opportunity for membrane surface charge measurements. The authors acknowledge financial support from the National Science Foundation CAREER grant (CBET-1552571) to MK for this work. Support was also provided through CBET-1705278 and DMR-1709522 for various aspects of this work.

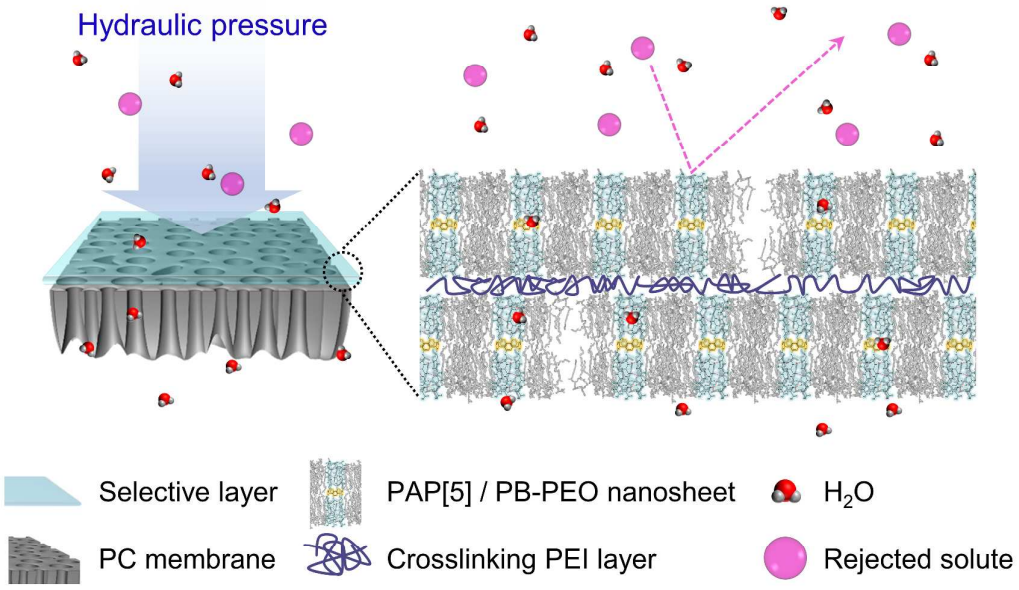

Figure 1. Schematic illustration of the ML-PAP[5] membrane structure. ML-PAP[5] membranes have thin selective layers on the top of porous support polycarbonate (PC) membrane. To form the defect free selective layer, PAP[5] nanosheets were laterally deposited and chemically cross-linkable PEI interlayers were introduced between PAP[5] nanosheets. Surfaces of PAP[5] nanosheets were terminated with -COOH groups so that these reactive groups can be exploited in peptide bond formation with -NH_2 groups of PEI polymers in order to confer structural stability to selective layers.

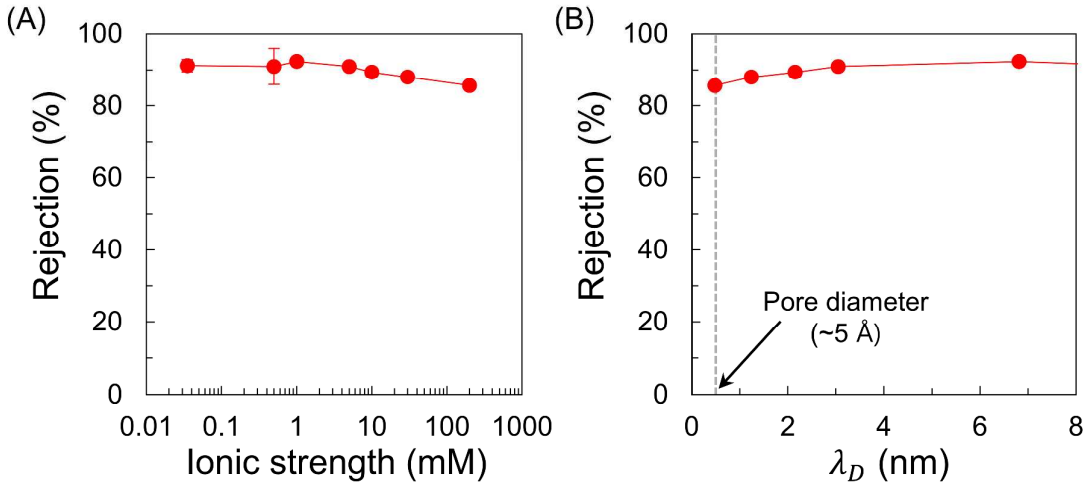

Figure 2. Methyl blue dye rejection as a function of (A) ionic strength and corresponding (B) Debye screening length (λ_D, nm) of solution. Methyl blue dyes were selected as a subject solute due to their comparable molecular weight (~750 Da) to the MWCO of the membranes (~500 Da). The ionic strength of solutions was adjusted using NaCl. Small error bars (smaller than 1%, n = 3) are not shown for clarity except for 0.5 mM in (A).

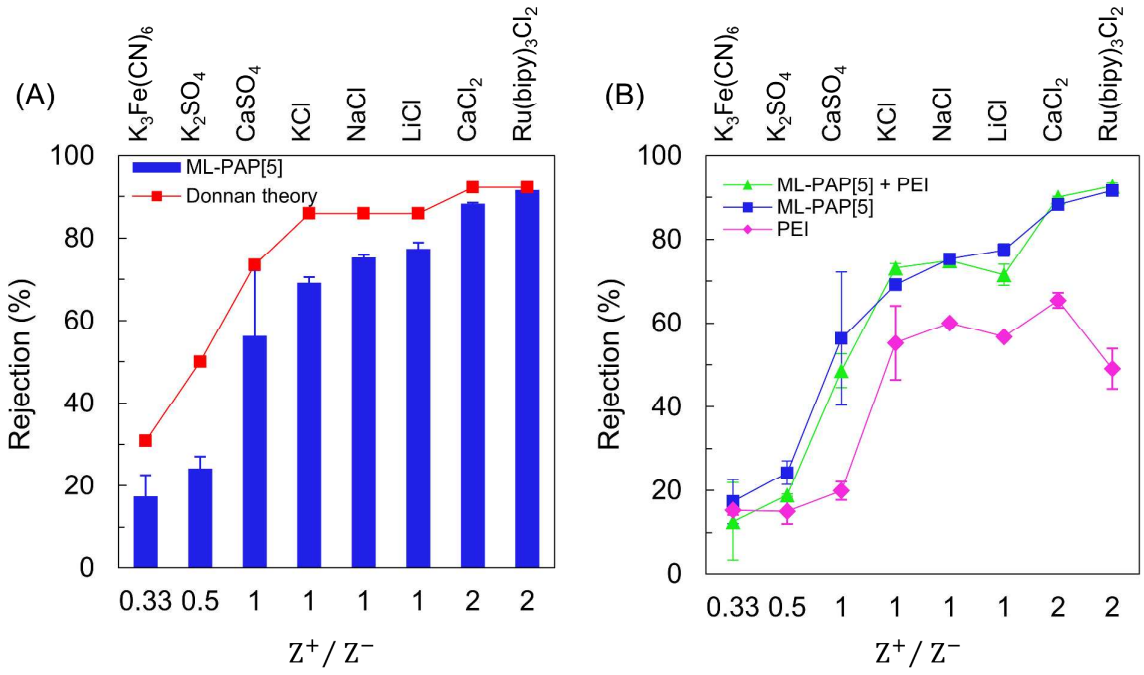

Figure 3. Point-charged ion rejection tests indicate the presence of a positively charged discriminating layer on the membrane. Z^+ and Z^- are ionic valence numbers of positive and negative charge ions respectively. (A) Ion rejection results of ML-PAP[5] membranes along with various valence ratios of positive to negative charge ions. Theoretical Donnan rejections were calculated using the equation (3). The membrane charge was estimated as 3.5 mM, obtained by fitting the experimental rejection data of $Ru(bipy)_3Cl_2$ salts into equation (3). (B) Ionic rejection trends of support membrane with only PEI layer (PEI), ML-PAP[5] membrane (ML-PAP[5]), and ML-PAP[5] membrane with additional PEI layer on the top (ML-PAP[5] + PEI). $K_3Fe(CN)_6$; potassium ferricyanide, K_2SO_4; potassium sulfate, $CaSO_4$; calcium sulfate, KCl; potassium chloride, NaCl; sodium chloride, LiCl; lithium chloride, $CaCl_2$; calcium chloride, and $Ru(bipy)_3Cl_2$; tris(bipyridine)ruthenium(III) chloride.

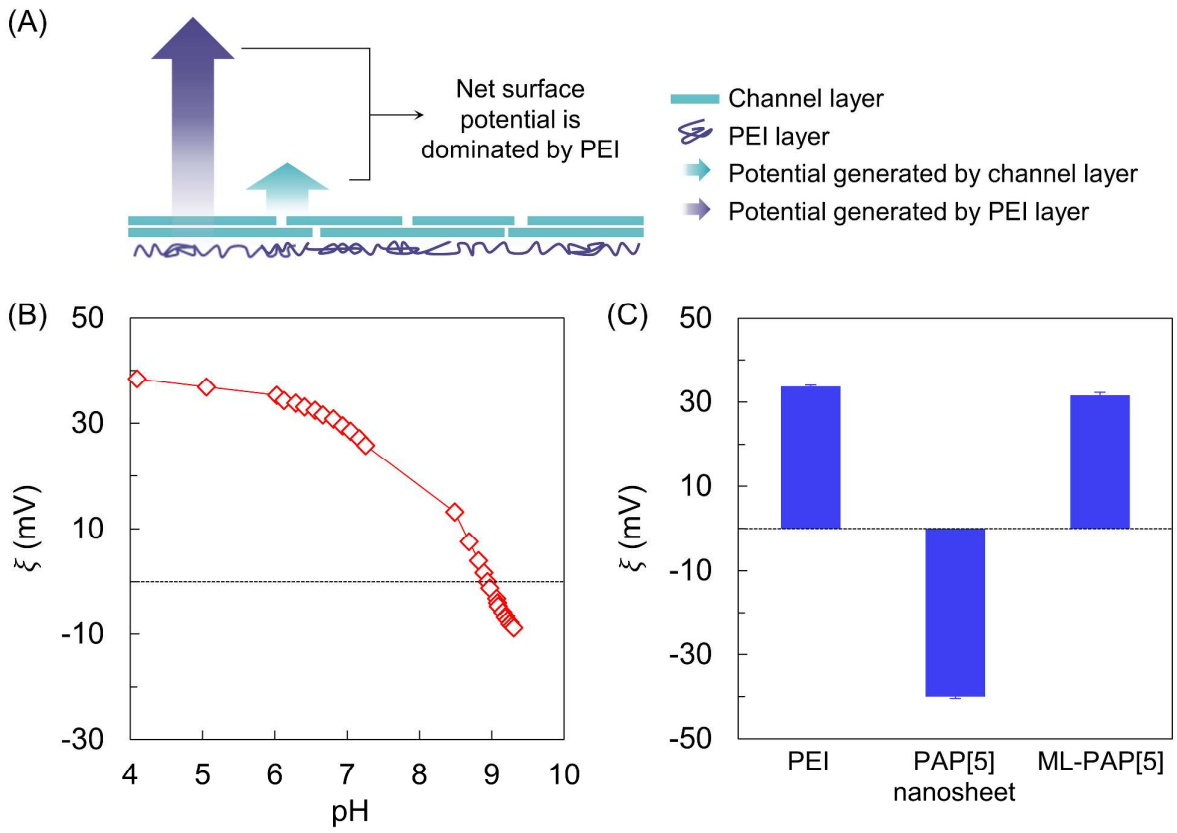

Figure 4. Zeta potential measurements confirm that the surface potential of the ML-PAP membranes is dominated by the positively charged PEI layers. (A) Schematic illustration for surface charge of ML-PAP[5] membranes. (B) Zeta potential (ξ, mV) measurements of ML-PAP[5] membranes were conducted at a wide range of pH values. These indicated that the isoelectric point was located around pH 9, indicating positively charged surface behavior of ML-PAP[5] membranes around circumneutral pH environments. (C) Zeta potentials of the membrane with only PEI layer (PEI), the membrane with only PAP[5] nanosheet layer (PAP[5] nanosheet), and ML-PAP[5] membrane (ML-PAP[5]) respectively at pH 6.5, which was representative of filtration testing conditions.

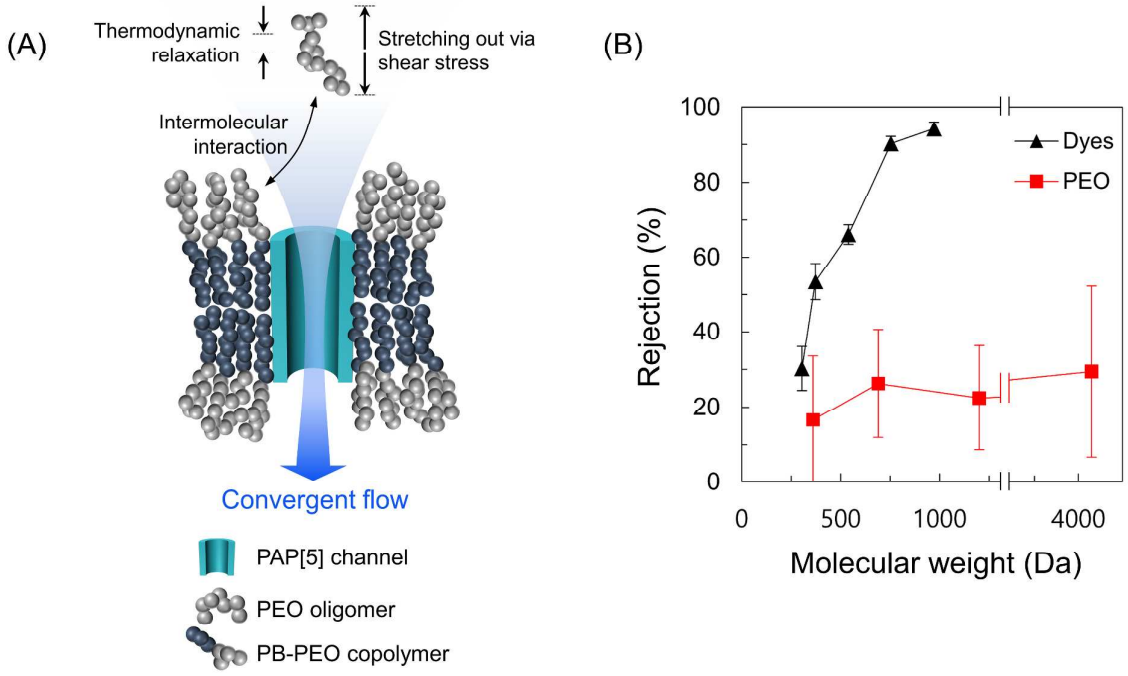

Figure 5. Several factors lead to passage of large MW linear PEO molecules through the straight through pore of the PB-PEO based ML-PAP membranes. (A) Schematic illustration of possible factors for PEO polymer deformation, entering into cylindrical PAP[5] water channel. (B) ML-PAP[5] membranes' rejection results of globular dyes and linear PEO polymers with wide molecular weight range.

References

1. H. B. Park, J. Kamcev, L. M. Robeson, M. Elimelech and B. D. Freeman, *Science*, 2017, **356**.
2. Y.-x. Shen, P. O. Saboe, I. T. Sines, M. Erbakan and M. Kumar, *Journal of Membrane Science*, 2014, **454**, 359-381.
3. E. Licsandru, I. Kocsis, Y. X. Shen, S. Murail, Y. M. Legrand, A. van der Lee, D. Tsai, M. Baaden, M. Kumar and M. Barboiu, *J Am Chem Soc*, 2016, **138**, 5403-5409.
4. Y. X. Shen, W. Si, M. Erbakan, K. Decker, R. De Zorzi, P. O. Saboe, Y. J. Kang, S. Majd, P. J. Butler, T. Walz, A. Aksimentiev, J. L. Hou and M. Kumar, *Proc Natl Acad Sci U S A*, 2015, **112**, 9810-9815.
5. R. H. Tunuguntla, R. Y. Henley, Y.-C. Yao, T. A. Pham, M. Wanunu and A. Noy, *Science*, 2017, **357**, 792.
6. Y.-x. Shen and M. Kumar, *AIChE Proceedings*, 2017.
7. F. Fornasiero, H. G. Park, J. K. Holt, M. Stadermann, C. P. Grigoropoulos, A. Noy and O. Bakajin, *Proceedings of the National Academy of Sciences*, 2008, **105**, 17250-17255.
8. F. G. Donnan, *Chemical Reviews*, 1924, **1**, 73-90.
9. H. Ohshima and S. Ohki, *Biophysical Journal*, 1985, **47**, 673-678.
10. J. Schaep, B. Van der Bruggen, C. Vandecasteele and D. Wilms, *Separation and Purification Technology*, 1998, **14**, 155-162.
11. F. Brochard and P. G. d. Gennes, *The Journal of Chemical Physics*, 1977, **67**, 52-56.
12. S. Daoudi and F. Brochard, *Macromolecules*, 1978, **11**, 751-758.
13. T. D. Long and J. L. Anderson, *Journal of Polymer Science: Polymer Physics Edition*, 1984, **22**, 1261-1281.
14. Q. T. Nguyen and J. Neel, *Journal of Membrane Science*, 1983, **14**, 111-127.
15. D. R. Latulippe and A. L. Zydney, *Journal of Membrane Science*, 2009, **329**, 201-208.
16. D. R. Latulippe, K. Ager and A. L. Zydney, *Journal of Membrane Science*, 2007, **294**, 169-177.
17. C. W. Hancher and A. D. Ryon, *Biotechnology and Bioengineering*, 1973, **15**, 677-692.
18. T. Hirasaki, T. Sato, T. Tsuboi, H. Nakano, T. Noda, A. Kono, K. Yamaguchi, K. Imada, N. Yamamoto, H. Murakami and S.-i. Manabe, *Journal of Membrane Science*, 1995, **106**, 123-129.
19. A. Higuchi, K. Kato, M. Hara, T. Sato, G. Ishikawa, H. Nakano, S. Satoh and S.-i. Manabe, *Journal of Membrane Science*, 1996, **116**, 191-197.
20. D. W. Kahn, M. D. Butler, D. L. Cohen, M. Gordon, J. W. Kahn and M. E. Winkler, *Biotechnology and Bioengineering*, 2000, **69**, 101-106.
21. E. J. Hinch, *The Physics of Fluids*, 1977, **20**, S22-S30.
22. H. S. Hsich, *Journal of Polymer Science Part C: Polymer Letters*, 1987, **25**, 511-512.
23. M. F. Jimenez-Solomon, Q. Song, K. E. Jelfs, M. Munoz-Ibanez and A. G. Livingston, *Nat Mater*, 2016, **15**, 760-767.
24. L. Xu, S. Shahid, J. Shen, E. A. C. Emanuelsson and D. A. Patterson, *Journal of Membrane Science*, 2017, **525**, 304-311.
25. R. Rohani, M. Hyland and D. Patterson, *Journal of Membrane Science*, 2011, **382**, 278-290.